Biochemical and Biophysical Research Communications 430 (2013) 1253–1258

Contents lists available at SciVerse ScienceDirect

Biochemical and Biophysical Research Communications

journal homepage: www.elsevier.com/locate/ybbrc

Structure of the complex of *Neisseria gonorrhoeae* *N*-acetyl-L-glutamate synthase with a bound bisubstrate analog

Gengxiang Zhao [a], Norma M. Allewell [b], Mendel Tuchman [a], Dashuang Shi [a,c,*]

[a] Center for Genetic Medicine Research and Department of Integrative Systems Biology, Children's National Medical Center, The George Washington University, Washington, DC 20010, USA

[b] Department of Cell Biology and Molecular Genetics and Department of Chemistry and Biochemistry, College of Computer, Mathematical, and Natural Sciences, University of Maryland, College Park, MD 20742, USA

[c] Key Laboratory of Organo-Pharmaceutical Chemistry, Jiangxi Province, Gannan Normal University, Ganzhou 341000, China

ARTICLE INFO

Article history:
Received 29 November 2012
Available online 20 December 2012

Keywords:
N-Acetyl-glutamate synthase
N-Acetyl-glutamate kinase
GCN5-acetyltransferase
Bisubstrate analog
Arginine biosynthesis

ABSTRACT

N-Acetyl-L-glutamate synthase catalyzes the conversion of AcCoA and glutamate to CoA and *N*-acetyl-L-glutamate (NAG), the first step of the arginine biosynthetic pathway in lower organisms. In mammals, NAG is an obligate cofactor of carbamoyl phosphate synthetase I in the urea cycle. We have previously reported the structures of NAGS from *Neisseria gonorrhoeae* (ngNAGS) with various substrates bound. Here we reported the preparation of the bisubstrate analog, CoA-*S*-acetyl-L-glutamate, the crystal structure of ngNAGS with CoA-NAG bound, and kinetic studies of several active site mutants. The results are consistent with a one-step nucleophilic addition–elimination mechanism with Glu353 as the catalytic base and Ser392 as the catalytic acid. The structure of the ngNAGS-bisubstrate complex together with the previous ngNAGS structures delineates the catalytic reaction path for ngNAGS.

© 2012 Elsevier Inc. All rights reserved.

1. Introduction

N-Acetyl-L-glutamate synthase (NAGS) catalyzes the first committed step in the arginine biosynthetic pathway in most microorganisms and plants, the acetylation of L-glutamate by AcCoA to produce *N*-acetyl-L-glutamate (NAG) [1,2]. Protein sequence comparison identified two major types of NAGS [3]. The first type, termed classical NAGS or bacterial-like NAGS, identified in most bacteria and plants, has an inactive amino acid kinase (AAK) domain and an active GCN5-like *N*-acetyltransferase (NAT) domain. The second type, termed vertebrate-like NAGS, has been identified in vertebrates, including mammals, and also in fungi and some bacteria. Since mutations in the human NAGS gene cause severe hyperammonia [4] understanding vertebrate-like NAGS has considerable clinical relevance.

Although vertebrate-like NAGS also consists of two domains, AAK and NAT domains, the NAT domain of this enzyme type seems to have evolved from different ancestors than bacterial-like NAGS, since the sequence identity of this domain is as low as 9–20%. Interestingly, fungal *N*-acetyl-glutamate kinases (NAGK), which also belong to this type, have an active AAK domain and an inactive NAT domain [5]. In some bacteria such as *Xanthomonas campestris* and *Maricaulis maris*, the two domains have both NAGS and NAGK catalytic activity, respectively. These enzymes are referred to as bifunctional NAGS/K [3,6], and they are thought to be the ancestral proteins for the present day vertebrate-like NAGS and fungal NAGK, which resulted from loss of NAGK activity in the AAK domain or NAGS activity in the NAT domain, respectively.

We have determined crystal structures of both vertebrate-like and bacterial-like NAGS. Bacterial NAGS from *Neisseria gonorrhoeae* [7,8] has a hexameric molecular architecture similar to those of arginine-sensitive NAGK enzymes [9]. The six monomers form a ring with two types of intersubunit interfaces: one similar to those in arginine insensitive NAGK enzymes such as *Escherichia coli* NAGK [10] involving adjacent AAK domains and a second formed by interlacing extended N-terminal helices of adjacent subunits. The six catalytic active sites are located in six NAT domains on opposite sides of the hexameric ring. Binding of the allosteric inhibitor, L-arginine, to the AAK domain at a site similar to those

Abbreviations: AAK, amino acid kinase; CoA-NAG, CoA-*S*-acetyl-L-glutamate; GNAT, GCN5-related acetyltransferase; mmNAGS/K, *Maricaulis maris* *N*-acetyl-L-glutamate synthase/kinase; NAG, *N*-Acetyl-L-glutamate; NAGK, *N*-Acetyl-L-glutamate kinase; NAGS, *N*-acetyl-L-glutamate synthase; NAGS/K, *N*-acetyl-L-glutamate synthase/kinase; NAT, *N*-acetyltransferase; ngNAGS, *Neisseria gonorrhoeae* *N*-acetyl-L-glutamate synthase; RMSD, root mean standard deviation; xcNAGS/K, *Xanthomonas campestris* *N*-acetyl-L-glutamate synthase/kinase.

* Corresponding author at: Center for Genetic Medicine Research and Department of Integrative Systems Biology, Children's National Medical Center, The George Washington University, 111 Michigan Avenue, N.W., Washington, DC 20010-2970, USA. Fax: +1 202 476 6014.

E-mail address: dshi@cnmcresearch.org (D. Shi).

0006-291X/$ - see front matter © 2012 Elsevier Inc. All rights reserved.
http://dx.doi.org/10.1016/j.bbrc.2012.12.064

found in arginine-sensitive NAGK enzymes, induces large conformational changes that enlarge and shorten the hexameric ring as seen in arginine-sensitive NAGK structures [9] and re-orients the NAT domain relative to the AAK domain by 109° [7]. As a result, a different surface of the NAT domain interacts with the AAK domain, the L-glutamate binding loops become disordered and enzyme activity decreases.

In contrast to the hexameric structure of bacterial-like NAGS, both bifunctional bacterial NAGS/K and NAGK in yeast exist as tetramers [5,11]. Tetramer formation involves dimeric interfaces between adjacent AAK domains and N-terminal helices as seen in bacterial-like NAGS, but the specific interactions are different. The AAK domain of yeast NAGK, without the NAT domain, is also a tetramer, implying that the AAK domain is likely to be key to tetramer formation [5]. However, in this type of NAGS, the NAT domains interact to enhance the tetramer architecture in contrast to bacterial-type NAGS in which NAT–NAT domains interactions are not seen.

The crystal structures of ngNAGS bound with various substrates that have been determined provide significant insights into the catalytic mechanism of bacterial-like NAGS enzymes. However, no other structures of NAGS/K enzymes with substrates bound have been reported, despite extensive efforts, perhaps because the affinity of these enzymes and other GCN5 related acetyltransferases (GNAT) [12] for AcCoA is significantly less that for ngNAG. However, bisubstrate analogs are often able to overcome such challenges because both substrate moieties contribute to binding.

Here we report the preparation of a bisubstrate analog, CoA-*S*-acetyl-L-glutamate (CoA-NAG), using the ngNAGS enzyme itself as the catalyst. The structure of ngNAGS complexed with the bisubstrate analog indicates that the bisubstrate analog binds to the active site similar to the way in which CoA and NAG bind separately, providing information about the intermediate reaction step. This structure, together, with biochemical analyses of several active site mutants provide further insights into the catalytic mechanism of bacterial-like NAGS enzymes. This strategy can be applied to structural and functional studies of the second type of NAGS enzymes, including human NAGS, whose deficiency causes hyperammonemia, as well as other members of the GNAT superfamily for which substrate bound structures are difficult to obtain.

2. Materials and methods

2.1. Materials and chemicals

All materials and chemicals except *N*-chloroacetyl-L-glutamate were commercially available. *N*-Chloroacetyl-L-glutamate was custom-made by Aris Pharmaceutical Inc (New Jersey).

2.2. Cloning and protein expression and purification

ngNAGS and all mutants were expressed and purified performed as described previously [8]. Briefly, the proteins were expressed in *E. coli* BL21(DE3) cells (Invitrogen) and purified with nickel affinity and DEAE columns (GE Healthcare). Protein purity was verified by SDS/PAGE gel and protein concentration was measured with a Nano-drop 1000 spectrophotometer (Thermo Scientific). An extinction coefficient of 25,900 $mol^{-1}cm^{-1}$ and molecular weight of 49.2 KDa obtained from the ExPASy web server (http://web.expasy.org/protparam/) were used to calculate protein concentrations. The protein was stored at 253 K in a buffer of 50 mM Tris–HCl, pH8.0, 50 mM NaCl, 10% glycerol, 5 mM β-mercaptoethonol, and 1 mM EDTA. Similar methods were used to over-express and purify *Maricaulis maris* NAGS (mmNAGS), *Xanthomonas campestris* NAGS (xcNAGS) and the mouse NAGS NAT domain (mNAGS), which contains mouse NAGS sequence from Met370 to Ser527.

2.3. Site-directed mutagenesis

Site-directed mutant genes of ngNAGS were created using primers containing the desired mutations (Table 1) and the QuikChange Mutagenesis Kit according to the manufacturer's protocol (Stratagene). The sequences of mutant DNA sequences were verified by DNA sequencing.

2.4. Activity assay

Enzymatic activity was assayed using the method described previously [13]. In brief, a stable isotope dilution method using liquid chromatography mass spectrometry (LC–MS) to measure NAG production was adopted. The assay was performed in a solution containing 50 mM Tris, pH 8.5, 10 mM glutamate and 2.5 mM AcCoA in a 100 μl reaction volume. The reaction was initiated by the addition of enzyme, and the mixture was incubated at 303 K for 5 min and quenched with 100 μl of 30% trichloroacetic acid containing 50 μg of *N*-acetyl-[$^{13}C_5$]glutamate as an internal standard. Precipitated protein was removed by micro-centrifugation. The supernatant (10 μl) was submitted to LC–MS (Agilent) for separation and measurement. The mobile phase consisted of 93% solvent A (1 ml trifluoroacetic acid in 1 L water) and 7% solvent B (1 ml trifluoroacetic acid in 1 L of 1:9 water/acetonitrile) and the flow rate is 0.6 ml/min. Glutamate, NAG, and ^{13}C-NAG were detected and quantified by selected ion monitoring mass spectrometry.

2.5. Detection of CoA-NAG bisubstrate analog

The LC–MS assay used to monitor activity was adapted to detect the formation of the CoA-NAG bisubstrate analog, using the similar standard reaction mixture: 100 μl of a solution containing 10 mM CoA, 10 mM *N*-chloroacetyl-L-glutamate, and 2 μg of ngNAGS in 100 mM Tris–HCl, pH 8.5. The reaction was performed at 303 K

Table 1
Diffraction data and refinement statistics.

Data collection	
Space group	P312
Wavelength (Å)	1.54178
Resolution (Å)	50–2.75
Highest resolution shell (Å)	2.8–2.75
Unit-cell parameters (Å)	a = 98.5 b = 98.5 c = 90.0
Measurements	128,602
Unique reflections	13,151 (647)
Redundancy	9.8 (9.7)
Completeness (%)	99.8 (100)[a]
R_{merg}[b]	0.087 (0.522)
$\langle I/\sigma(I)\rangle$	12.9 (1.6)
Refinement	
Reflections, working set	13,149 (1,179)
Reflections, test set	1,331 (134)
Total atom (non-H)	3.327
Protein atoms	3,227
Ligand atoms	66
Water atoms	34
R	0.189 (0.367)
R_{free}	0.271 (0.414)
Rmsd bond lengths (Å)	0.008
Rmsd bond angles (°)	1.188

[a] Figures in brackets apply to the highest-resolution shell.
[b] $R_{merg} = \Sigma_h\Sigma_i|I(h,i) - \langle I(h)\rangle|/\Sigma_h\Sigma_i I(h,i)$, where $I(h,i)$ is the intensity of the ith observation of reflection h, and $\langle I(h)\rangle$ is the average intensity of redundant measurements of reflection h.

Table 2
Mutation-engineering primers.

Mutants	Primers
E355A	GAAGCCGATTGCGGC**GCA**ATCGCCTGCCTTGCC
E355D	GAAGCCGATTGCGGC**GAT**ATCGCCTGCCTTGCC
S392A	AGGCTG TTCGCACTG**GCC**ACAAATACCGGCGAA

for 5 min. After the reaction, protein was removed by boiling the sample for 10 min and centrifuging for 5 min. The supernatant (10 μl) was submitted to LC–MS to detect the CoA-NAG bisubstrate analog using selected ion monitoring mass (*m/z* 955) spectrometry. The same procedure was used with NAGS from different organisms including mmNAGS, xcNAGS and mNAGS (NAT domain only).

2.6. Crystallization

Purified ngNAGS was concentrated to 10 mg/ml with an Amicon-Y30 membrane concentrator (Millipore). Before crystallization, ngNAGS was incubated with 10 mM CoA and 10 mM *N*-chloroacetyl-L-glutamate for 30 min. Screening for crystallization conditions was performed using sitting-drop vapor diffusion in 96-well plates (Hampton Research) at 291 K by mixing 2 μl of the protein solution with 2 μl of the reagent solution from the sparse matrix Crystal Screens 1 and 2, and Index Screen (Hampton Research). The best crystals reported here were grown from a well solution containing 100 mM tri-Na citrate, pH5.6, 0.2 M $MgCl_2$ and 8% PEG 3350 by the sitting-drop vapor-diffusion method.

2.7. Data collection and structure determination

Before data collection, crystals were transferred from the crystallization plate to a well solution supplemented with 20% glycerol and then frozen directly by a liquid nitrogen stream (Oxford). Diffraction data were collected at the NIDDK Molecular Structure Facility using a Rigaku Raxis-IV+ and CCD detector. All data were processed using the HKL2000 package [14]; statistics are summarized in Table 2. After several cycles of refinements with Phenix [15] and model adjustments with Coot [16], the final *R* and R_{free} were 18.9% and 27.1%, respectively. Refinement statistics for the final refined model are given in Table 1. The final refined coordinates for bisubstrate analog bound ngNAGS have been deposited in RCSB Protein Data Bank with accession codes, 4I49.

3. Results and discussion

3.1. Preparation of bisubstrate analog

Most bisubstrate analogs used in structural and functional studies have been prepared using chemical methods; for examples, *N*-phosphonacetyl-L-aspartate for aspartate transcarbamylase [17] and the bisubstrate inhibitors for MYST, HATs, Esa1 and Tip60 [18]. Sometimes bacteria can make bisubstrate analogs using biosynthetic pathways encoded in their genome such as (*R*)-N^{δ}-(*N*′-sulfodiaminophosphinyl)-L-ornithine, which is produced from *Pseudomonas savastanoi pv. phaseolicola* [19]. Recently, a method that uses the enzyme itself as the catalyst to make a bisubstrate analog has been developed [20]. In this approach, chloroacetyl-CoA was synthesized, and then the other substrate and the enzyme were added to make the conjugated bisubstrate analog, CoA-*S*-acetyl-substrate. This method has been successfully used in structural and functional studies of several acetyltransferases including spermidine/spermine *N*-acetyltransferase [21] and RimI, which acetylates ribosomal protein S18 [12]. The reaction proceeds in two steps. Initially, a chloroacetyl group is transferred from chloroacetyl-CoA to the substrate, which then reacts further with CoA to form CoA-*S*-acetyl-substrate. In our study, we adapted this method and used CoA and *N*-chloroacetyl-L-glutamate as the starting materials. Our LC–MS experiments confirmed that the bisubstrate analog, CoA-NAG can be easily made using ngNAGS, xcNAGS, mmNAGS, and even the NAT domain of mouse NAGS to catalyze the reaction (Fig. 1).

3.2. Structure of ngNAGS bound with CoA-S-acetyl-L-glutamate

To gain further insight into the catalytic mechanism and molecular basis of the binding of the bisubstrate analog to ngNAGS, CoA and *N*-chloroacetyl-L-glutamate were added to a solution of

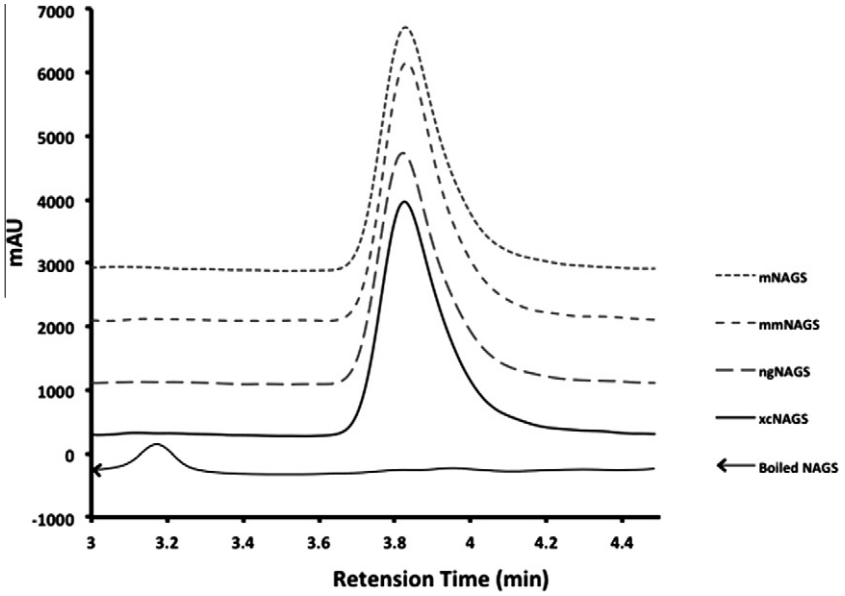

Fig. 1. LC–MS analysis of the enzymatically synthesized bisubstrate analog, CoA-NAG. Production of CoA-NAG was monitored by select ion mass (*m/z* 955) spectrometry. Samples with boiled ngNAGS are shown as a solid trace with arrow; unboiled xcNAGS as a solid trace; ngNAGS as a long dashed trace; mmNAGS as a short dashed trace; mouse NAGS NAT domain only (mNAGS) as the shortest dashed trace. Traces for different samples are shown offset vertically.

ngNAGS which was then crystallized in space group P321 with unit-cell parameters $a = b = 98.5$ and $c = 90.1$ Å, isomorphous to the ngNAGS structures without L-arginine bound [8]. Superimposition of the structure of the bisubstrate-ngNAGS complex with acetyl-CoA-ngNAGS (PDB: 2R8V), CoA-Glu-ngNAGS (PDB: 3D2M) and CoA-NAG-ngNAGS (PDB: 3B8G) results in RMSD of 0.47, 0.37 and 0.35 Å, respectively and indicates the close similarity among these structures.

3.3. Bisubstrate analog binding

The electron density for the bisubstrate analog is well defined (Fig. 2A) and the interactions between the bisubstrate analog and protein can be unambiguously identified (Fig. 2B). The CoA moiety of the bisubstrate analog binds to the protein *via* hydrogen bonding interactions with the main-chain nitrogen atoms of Cys356, Leu357, Asp365, Gly369, Glu370, Gly366 and Gly367, and the main-chain oxygen atoms of Leu357 and Asn394. The side-chain atoms of Ser392, Thr359, Trp398, Glu397, and Arg151 and Lys152 from the adjacent subunit are also involved in binding the CoA moiety. Since the sulfur atom of the CoA moiety links to the methyl carbon atom of acetyl group directly, its sulfur atom is shifted toward towards the β-strand, B23, by about 1.3 Å, relative to the structure with CoA bound alone. However, the carbonyl oxygen atom of the acetyl group still points to the β-bulge formed in β-strand, B22, at residues Cys356 and Leu357, and forms hydrogen bonds with their main-chain nitrogen atoms. Since the β-bulge structure and their hydrogen bonding interaction with the acetyl group are conserved in all known GNAT structures, this feature appears likely to function in catalysis by polarizing the carbonyl bond to facilitate the attack of the incoming amino nitrogen atom of the second substrate. Interactions between the protein and the NAG moiety of CoA-NAG are very similar to those observed in the CoA-Glu-ngNAGS and CoA-NAG-ngNAGS structures. In all cases, NAG is positioned with its α-carboxyl group anchored by the main-chain nitrogen atom of Cys356 and the side-chain of Arg316, and the position of the γ-carboxyl group is fixed by interactions with the side-chains of Arg416, Arg425 and Ser427 and the α-amino nitrogen atom is secured by hydrogen bonding interactions with the main-chain oxygen atom of Leu391.

3.4. Comparison of the kinetic parameters of S392A, E353A, E353D and wild-type ngNAGS

ngNAGS appears to use a one-step direct transfer mechanism for the catalytic reaction because there is not a suitable cysteine nearby for a two-step ping-pong catalytic mechanism [8]. In order to probe the possible functional roles of nearby residues, several active site mutants were made and their specific activities were determined (Table 3). The mutant S392A has 18-fold lower specific activity than the wild-type enzyme, consistent with the potential functional role of S392 as general acid as proposed previously for

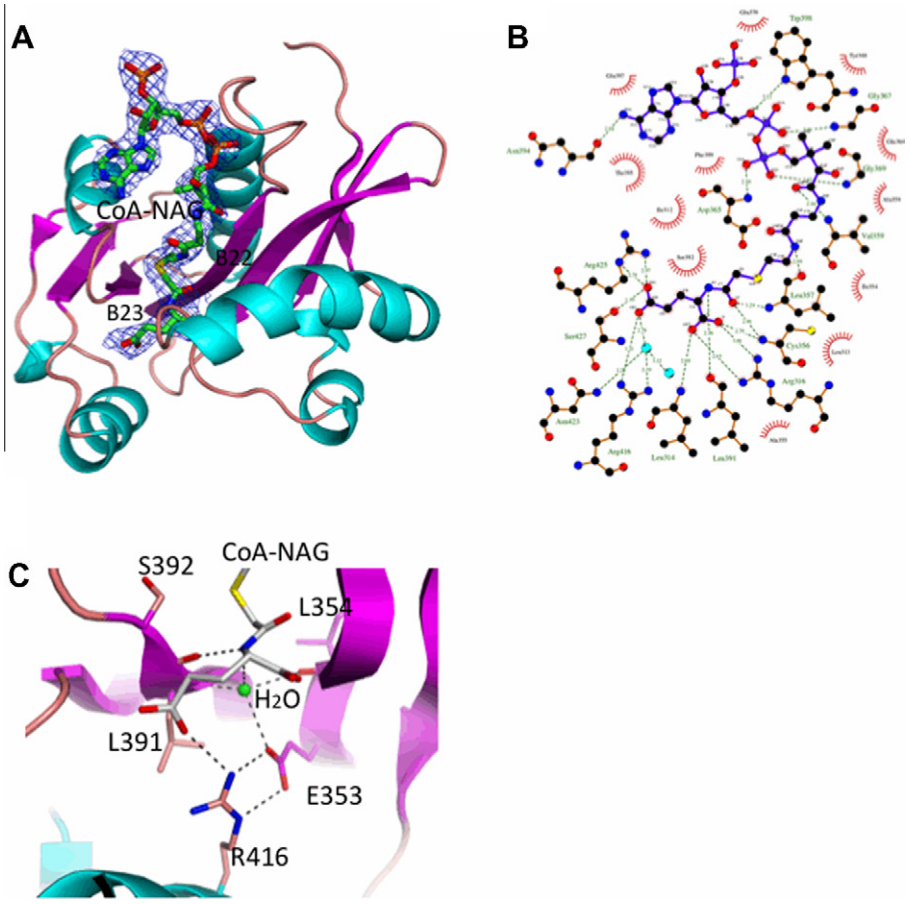

Fig. 2. Interactions of CoA-NAG with ngNAGS. (A) Ribbon diagram of ngNAGS NAT domain with CoA-NAG bound. The *pink arrows* indicate the direction of strands in β-sheets, α-helices are in *light blue*, and β-sheets are in *green*. The electron density map (2Fo _ Fc) (1.0σ shown as a *blue cage*) corresponds to bound CoA-NAG. The carbon atoms of CoA-NAG are shown as *green sticks*. (B) Detailed schematic of interactions of the bisubstrate analog CoA-NAG with ngNAGS. (C) Interactions of the conserved water molecule with the *N*-amino group of NAG moiety and the side chain of Glu353. The protein is shown in pink (β-sheet) and light blue (α-helices) ribbons. CoA-NAG and the side chains of residues discussed in the text are shown as sticks. The hydrogen bonds are shown as dashed lines. Figures were drawn using programs Pymol [33] and Ligplot [34].

Table 3
Specific enzymatic activity of wild-type ngNAGS and its mutants.

Proteins	Specific activity ($\mu mol\ min^{-1}\ mg^{-1}$)
Wide-type	28.02 ± 1.39[a]
E353A	8.42 ± 0.97
E353D	0.99 ± 0.01
S392A	1.54 ± 0.10

[a] Specific activity is the average of three measurements with its standard deviation.

ngNAGS [7,8] as well for other GCN5 related acetyltransferases (GNAT) [12]. E353A and E353D have 3.5-fold and 28.4-fold lower specific activities than the wild-type enzyme, respectively, demonstrating that Glu353 has a significant role in the enzyme reaction. Since Glu353 helps to orient the glutamate binding residue Arg416, on one hand, and to form a "proton wire" that accepts a proton from the amino group of glutamate *via* a water molecule, on the other hand, it appears to play double roles, assisting in binding the substrate, and acting as a proton acceptor (Fig. 2C). Interestingly, the E353A mutant has significant higher specific activity than E353D. It is possible that another water molecule or other small molecule occupies the space left by E392A and restores the role of the carboxyl group of E353, as has been observed in other mutant studies [22].

3.5. Catalytic mechanism and potential catalytic residues

Most members of the GNAT superfamily use a one-step catalytic mechanism for the catalytic reaction [23,24]. In this mechanism, an amino nitrogen atom attacks the carbon atom of the acetyl group of AcCoA to form a tetrahedral intermediate. The collapse of this intermediate results in the products, CoA and the acetylated substrate. During this catalytic process, at least one residue functioning as a general base may be required to facilitate the deprotonation of the attacking amino group. Various candidates have been proposed for the catalytic base in members of the GNAT superfamily including glutamate [12,25,26], histidine [27] or serine [28]. In the ngNAGS structures, a conserved glutamate residue, Glu353, is located at 5.6 Å from the attacking α-amino group of L-glutamate, but a conserved water molecule identified in all ngNAGS structures links the attacking α-amino group of L-glutamate to the side-chain of Glu353 *via* hydrogen bonding interactions. This intervening water molecule is held in the correct geometry by the carbonyl oxygen of Leu354 and the amide nitrogen of Leu391 to allow proton transfer from the attacking α-amino group of L-glutamate to Glu353 (Fig. 2C). Similar general bases, which interact with the attacking amino group *via* a water molecule, have been identified in other members of GNAT superfamily [12,25,26]. Since Glu353 also interacts with the L-glutamate binding residue, Arg416, through hydrogen bonds, it will also affect L-glutamate binding. Kinetic studies of the E353A mutant demonstrate that it has significantly lower activity, consistent with the proposed functional role.

In the catalytic reaction, a residue functioning as a general acid may also be required to protonate the product CoA. In most members of the GNAT superfamily, the general acid is usually a tyrosine, whose side-chain points to the sulfur atom of AcCoA [29]. However, the equivalent residue in ngNAGS is a phenylalanine (Phe399), which cannot function as a general acid. Instead, in the ngNAGS-bisubstrate complex structure, a serine, Ser392, is close to the sulfur atom of the bisubstrate analog (4.0 Å). In the CoA-ngNAGS complex structures [7,8], the side-chain of Ser392 hydrogen bonds with the thiol group of CoA (3.3 Å). Therefore, it is likely that Ser392 helps to protonate the thiol group of CoA and plays a role similar to a tyrosine in other members of GCN5 family. Our mutagenesis studies confirm the proposed catalytic role for Ser392 since the S392A mutant has significantly lower activity. Indeed, in other members of GCN5 superfamily in which no suitable tyrosine is available to function as a general acid, a nearby serine also plays a similar role [28].

The structural data in combination with the kinetic data for the mutants allow us to propose a detailed catalytic mechanism for ngNAGS (Fig. 3). Like other members of the GNAT superfamily, ngNAGS catalyzes the direct transfer of the acetyl group of AcCoA to the α-amino group of L-glutamate. Before the reaction, a glutamate, Glu353, acts as a general base *via* a water molecule to facilitate the deprotonation of the α-amino group of L-glutamate. Direct nucleophilic attack on the acetyl group of AcCoA by the neutral α-amino group of L-glutamate results in a tetrahedral intermediate, which may be stabilized by the polarization of the acetyl group *via* a hydrogen bonding interaction with the main-chain nitrogen atoms of Cys356 and Leu357. Collapse of the tetrahedral intermediate results in NAG and CoA. In the reaction, a serine, Ser392, may act as a general base to play a similar role to tyrosine in other members of the GNAT superfamily to assist in the protonation of the thiol group of CoA.

3.6. General application for other members of GCN5 family

The strategy of preparing bisubstrate analogs using the enzyme itself as a catalyst has been applied to spermidine/spermine

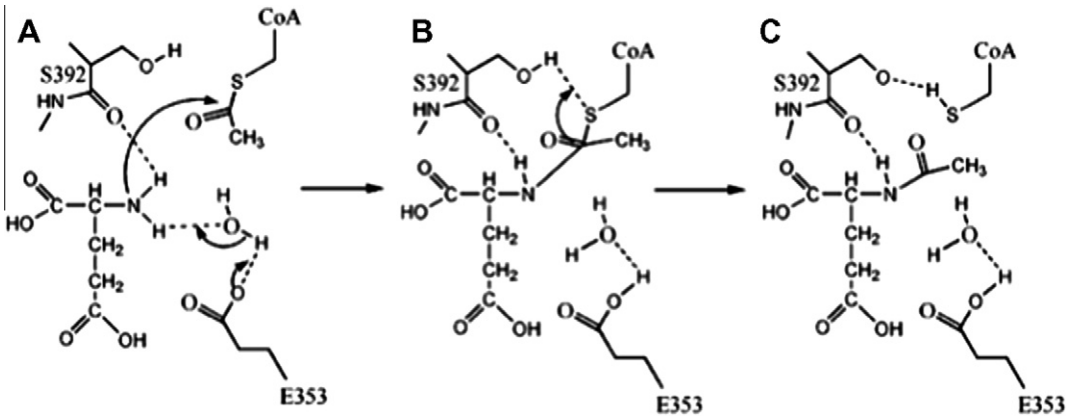

Fig. 3. Proposed reaction mechanism. (A) Schematic diagram showing the ternary complex, nucleophilic attack on the carbonyl carbon of AcCoA by the amino group of L-glutamate. Glu353 facilitates the deprotonation of the amino group of L-glutamate via the conserved water. (B) Schematic diagram the collapse of the tetrahedral intermediate. (C) Schematic diagram showing product formation and protonation of the thiol group of CoA by Ser392.

N-acetyltransferase [21], RimI for *N*-acetylation of ribosomal protein S18 [12] and ngNAGS. The method may also be used to prepare bisubstrate analogs of other members of the GCN5 superfamily including members of the MYST family such as histone acetyltransferase, serotonin *N*-acetyltransferase and aminoglycoside 6′-*N*-acetyltransferse, since bisubstrate analogs have already been prepared biochemically using chloroacetyl-substrates as starting materials [18,30–32].

Acknowledgments

This work was supported by Public Health Service grants DK-DK064913 (MT) and DK-067935 (DS) from the National Institute of Diabetes, Digestive and Kidney Diseases and HD32652 from the National Institute of Child Health and Human Development. We thank Dr. David Davies for facilitating the use of the diffraction equipment in the Molecular Structure Section of the National Institutes of Health and Dr. Fred Dyda for help in data collection.

References

[1] R. Cunin, N. Glansdorff, A. Pierard, V. Stalon, Biosynthesis and metabolism of arginine in bacteria, Microbiol. Rev. 50 (1986) 314–352.
[2] R.D. Slocum, Genes, enzymes and regulation of arginine biosynthesis in plants, Plant Physiol. Biochem. 43 (2005) 729–745.
[3] Q. Qu, H. Morizono, D. Shi, M. Tuchman, L. Caldovic, A novel bifunctional *N*-acetylglutamate synthase-kinase from *Xanthomonas campestris* that is closely related to mammalian *N*-acetylglutamate synthase, BMC Biochem. 8 (2007) 4.
[4] L. Caldovic, H. Morizono, M. Tuchman, Mutations and polymorphisms in the human *N*-acetylglutamate synthase (NAGS) gene, Hum. Mutat. 28 (2007) 754–759.
[5] S. de Cima, F. Gil-Ortiz, M. Crabeel, I. Fita, V. Rubio, Insight on an arginine synthesis metabolon from the tetrameric structure of yeast acetylglutamate kinase, PLoS One 7 (2012) e34734.
[6] D. Shi, L. Caldovic, Z. Jin, X. Yu, Q. Qu, L. Roth, H. Morizono, Y. Hathout, N.M. Allewell, M. Tuchman, Expression, crystallization and preliminary crystallographic studies of a novel bifunctional *N*-acetylglutamate synthase/kinase from *Xanthomonas campestris* homologous to vertebrate *N*-acetylglutamate synthase, Acta Crystallogr. Sect. F Struct. Biol. Cryst. Commun. 62 (2006) 1218–1222.
[7] L. Min, Z. Jin, L. Caldovic, H. Morizono, N.M. Allewell, M. Tuchman, D. Shi, Mechanism of allosteric inhibition of *N*-acetyl-L-glutamate synthase by L-arginine, J. Biol. Chem. 284 (2009) 4873–4880.
[8] D. Shi, V. Sagar, Z. Jin, X. Yu, L. Caldovic, H. Morizono, N.M. Allewell, M. Tuchman, The crystal structure of *N*-acetyl-L-glutamate synthase from *Neisseria gonorrhoeae* provides insights into mechanisms of catalysis and regulation, J. Biol. Chem. 283 (2008) 7176–7184.
[9] S. Ramon-Maiques, M.L. Fernandez-Murga, F. Gil-Ortiz, A. Vagin, I. Fita, V. Rubio, Structural bases of feed-back control of arginine biosynthesis, revealed by the structures of two hexameric *N*-acetylglutamate kinases, from Thermotoga maritima and Pseudomonas aeruginosa, J. Mol. Biol. 356 (2006) 695–713.
[10] S. Ramon-Maiques, A. Marina, F. Gil-Ortiz, I. Fita, V. Rubio, Structure of acetylglutamate kinase, a key enzyme for arginine biosynthesis and a prototype for the amino acid kinase enzyme family, during catalysis, Structure 10 (2002) 329–342.
[11] D. Shi, Y. Li, J. Cabrera-Luque, Z. Jin, X. Yu, G. Zhao, N. Haskins, N.M. Allewell, M. Tuchman, A Novel *N*-acetylglutamate synthase architecture revealed by the crystal structure of the bifunctional enzyme from *Maricaulis maris*, PLoS One 6 (2011) e28825.
[12] M.W. Vetting, D.C. Bareich, M. Yu, J.S. Blanchard, Crystal structure of RimI from Salmonella typhimurium LT2, the GNAT responsible for N(alpha)-acetylation of ribosomal protein S18, Protein Sci. 17 (2008) 1781–1790.
[13] L. Caldovic, H. Morizono, X. Yu, M. Thompson, D. Shi, R. Gallegos, N.M. Allewell, M.H. Malamy, M. Tuchman, Identification, cloning and expression of the mouse *N*-acetylglutamate synthase gene, Biochem. J. 364 (2002) 825–831.
[14] Z. Otwinowski, W. Minor, Processing of X-ray diffraction data collected in oscillation mode, Methods Enzymol. 276 (1997) 307–326.
[15] P.D. Adams, P.V. Afonine, G. Bunkoczi, V.B. Chen, I.W. Davis, N. Echols, J.J. Headd, L.W. Hung, G.J. Kapral, R.W. Grosse-Kunstleve, A.J. McCoy, N.W. Moriarty, R. Oeffner, R.J. Read, D.C. Richardson, J.S. Richardson, T.C. Terwilliger, P.H. Zwart, PHENIX: a comprehensive Python-based system for macromolecular structure solution, Acta Crystallogr. D Biol. Crystallogr. 66 (2010) 213–221.
[16] P. Emsley, K. Cowtan, Coot: model-building tools for molecular graphics, Acta Crystallogr. D Biol. Crystallogr. 60 (2004) 2126–2132.
[17] K.L. Krause, K.W. Volz, W.N. Lipscomb, Structure at 2.9-A resolution of aspartate carbamoyltransferase complexed with the bisubstrate analogue *N*-(phosphonacetyl)-L-aspartate, Proc. Natl. Acad. Sci. USA 82 (1985) 1643–1647.
[18] J. Wu, N. Xie, Z. Wu, Y. Zhang, Y.G. Zheng, Bisubstrate Inhibitors of the MYST HATs Esa1 and Tip60, Bioorg. Med. Chem. 17 (2009) 1381–1386.
[19] M.D. Templeton, L.A. Reinhardt, C.A. Collyer, R.E. Mitchell, W.W. Cleland, Kinetic analysis of the L-ornithine transcarbamoylase from *Pseudomonas savastanoi pv*. phaseolicola that is resistant to the transition state analogue (R)-N delta-(*N*′-sulfodiaminophosphinyl)-L-ornithine, Biochemistry 44 (2005) 4408–4415.
[20] M. Yu, M.L. Magalhaes, P.F. Cook, J.S. Blanchard, Bisubstrate inhibition: Theory and application to *N*-acetyltransferases, Biochemistry 45 (2006) 14788–14794.
[21] S.S. Hegde, J. Chandler, M.W. Vetting, M. Yu, J.S. Blanchard, Mechanistic and structural analysis of human spermidine/spermine N1-acetyltransferase, Biochemistry 46 (2007) 7187–7195.
[22] Y. Li, X. Yu, J. Ho, D. Fushman, N.M. Allewell, M. Tuchman, D. Shi, Reversible post-translational carboxylation modulates the enzymatic activity of *N*-acetyl-L-ornithine transcarbamylase, Biochemistry 49 (2010) 6887–6895.
[23] F. Dyda, D.C. Klein, A.B. Hickman, GCN5-related *N*-acetyltransferases: a structural overview, Annu. Rev. Biophys. Biomol. Struct. 29 (2000) 81–103.
[24] M.W. Vetting, L.P. de Carvalho, S.L. Roderick, J.S. Blanchard, A novel dimeric structure of the RimL Nalpha-acetyltransferase from Salmonella typhimurium, J. Biol. Chem. 280 (2005) 22108–22114.
[25] K.G. Tanner, R.C. Trievel, M.H. Kuo, R.M. Howard, S.L. Berger, C.D. Allis, R. Marmorstein, J.M. Denu, Catalytic mechanism and function of invariant glutamic acid 173 from the histone acetyltransferase GCN5 transcriptional coactivator, J. Biol. Chem. 274 (1999) 18157–18160.
[26] M.R. Langer, K.G. Tanner, J.M. Denu, Mutational analysis of conserved residues in the GCN5 family of histone acetyltransferases, J. Biol. Chem. 276 (2001) 31321–31331.
[27] A.B. Hickman, M.A. Namboodiri, D.C. Klein, F. Dyda, The structural basis of ordered substrate binding by serotonin *N*-acetyltransferase: enzyme complex at 1.8 A resolution with a bisubstrate analog, Cell 97 (1999) 361–369.
[28] K.C. Cheng, J.N. Liao, P.C. Lyu, Crystal structure of the dopamine *N*-acetyltransferase-acetyl-CoA complex provides insights into the catalytic mechanism, Biochem. J. 446 (2012) 395–404.
[29] H. He, Y. Ding, M. Bartlam, F. Sun, Y. Le, X. Qin, H. Tang, R. Zhang, A. Joachimiak, J. Liu, N. Zhao, Z. Rao, Crystal structure of tabtoxin resistance protein complexed with acetyl coenzyme A reveals the mechanism for beta-lactam acetylation, J. Mol. Biol. 325 (2003) 1019–1030.
[30] M.L. Magalhaes, M.W. Vetting, F. Gao, L. Freiburger, K. Auclair, J.S. Blanchard, Kinetic and structural analysis of bisubstrate inhibition of the Salmonella enterica aminoglycoside 6′-*N*-acetyltransferase, Biochemistry 47 (2008) 579–584.
[31] E. Wolf, J. De Angelis, E.M. Khalil, P.A. Cole, S.K. Burley, X-ray crystallographic studies of serotonin *N*-acetyltransferase catalysis and inhibition, J. Mol. Biol. 317 (2002) 215–224.
[32] A.N. Poux, M. Cebrat, C.M. Kim, P.A. Cole, R. Marmorstein, Structure of the GCN5 histone acetyltransferase bound to a bisubstrate inhibitor, Proc. Natl. Acad. Sci. USA 99 (2002) 14065–14070.
[33] L. Schrodinger, The PyMOL Molecular Graphics System, version 1.3r1, 2010.
[34] A.C. Wallace, R.A. Laskowski, J.M. Thornton, LIGPLOT: a program to generate schematic diagrams of protein-ligand interactions, Protein Eng. 8 (1995) 127–134.